Commun. Theor. Phys. **60** (2013) 363–374 Vol. 60, No. 3, September 15, 2013

Solution Space Coupling in the Random *K*-Satisfiability Problem*

ZENG Ying (曾颖) and ZHOU Hai-Jun (周海军)

State Key Laboratory of Theoretical Physics, Institute of Theoretical Physics, Chinese Academy of Sciences, Zhong-Guan-Cun East Road 55, Beijing 100190, China

(Received March 6, 2013; revised manuscript received May 13, 2013)

Abstract *The random K-satisfiability (K-SAT) problem is very difficult when the clause density is close to the satisfiability threshold. In this paper we study this problem from the perspective of solution space coupling. We divide a given difficult random K-SAT formula into two easy sub-formulas and let the two corresponding solution spaces to interact with each other through a coupling field x. We investigate the statistical mechanical property of this coupled system by mean field theory and computer simulations. The coupled system has an ergodicity-breaking (clustering) transition at certain critical value x_d of the coupling field. At this transition point, the mean overlap value between the solutions of the two solution spaces is very close to* 1. *The mean energy density of the coupled system at its clustering transition point is less than the mean energy density of the original K-SAT problem at the temperature-induced clustering transition point. The implications of this work for designing new heuristic K-SAT solvers are discussed.*

PACS numbers: 89.70.Eg, 75.10.Nr, 64.60.De
Key words: constraint satisfaction, spin glass, clustering transition, belief propagation, solution space

1 Introduction

The random K-satisfiability (K-SAT) problem is a fundamental problem in the field of computational complexity.[1−3] The solution space statistical property of the random K-SAT problem has been intensively studied by researchers from the statistical physics community in the last twenty years.[4−6] Deep insights on the evolution of the solution space structure have been achieved by the mean field theory of spin glasses.[5,7−9]

An instance (or formula) of the random K-SAT problem is composed of N binary (spin) variables and M clauses, with each clause being a constraint over K randomly chosen variables. The random K-SAT problem is controlled by a single structural parameter, the clause density $\alpha \equiv M/N$. On average each variable is constrained by $K\alpha$ clauses. The satisfiability threshold of the random K-SAT problem, $\alpha_s(K)$, marks the critical value of clause density beyond which it is impossible to satisfy simultaneously all the clauses of a large random K-SAT formula. The value of $\alpha_s(K)$ has been estimated by the mean field theory. For example, $\alpha_s(3) \approx 4.267$ and $\alpha_s(4) \approx 9.931$.[10] For $\alpha < \alpha_s(K)$, the non-empty solution space of a random K-SAT formula is formed by all the configurations of the N variables that satisfy simultaneously all the M clauses. This solution space experiences an ergodicity-breaking (or clustering) transition at a critical clause density $\alpha_d(K)$. The value of $\alpha_d(K)$ has also been estimated by the mean field theory, for example, $\alpha_d(3) \approx 3.86$ and $\alpha_d(4) \approx 9.38$.[9,11−12]

The random K-SAT problem in the clause density interval $\alpha \in [\alpha_d(K), \alpha_s(K)]$ is not easy to solve, especially for formulas with α very close to the satisfiability threshold $\alpha_s(K)$.[8,13−15] At $\alpha \approx \alpha_s(K)$, the solutions of a random K-SAT formula are distributed into many tiny clusters, these solution clusters are widely separated, and within each solution cluster a large number of variables have fixed spin values (the so-called freezing situation[16−17]) At $\alpha \approx \alpha_s(K)$ even the most powerful algorithm, the survey propagation algorithm,[8] fails to find solutions (for example, it works for $\alpha < 4.25$ for the random 3-SAT problem).

In this paper we study the random K-SAT problem from the viewpoint of solution space coupling. We distribute the $M = \alpha N$ clauses of a random K-SAT formula F into two sub-formulas F_1 and F_2 and let each sub-formula contain half of the clauses. The clause density α of the original formula F is close to $\alpha_s(K)$ and its solution space (denoted as $\mathcal{S}$) has a very complicated structure. Since each sub-formula has a much smaller clause density $\alpha' = \alpha/2 < \alpha_d(K)$, it is very easy to solve and its solution space (denoted as $\mathcal{S}_1$ for F_1 and $\mathcal{S}_2$ for F_2) is ergodic and relatively simple. The solution space $\mathcal{S}$ is the intersection of $\mathcal{S}_1$ and $\mathcal{S}_2$. We then apply a coupling field x between the solution spaces $\mathcal{S}_1$ and $\mathcal{S}_2$ and study how the statistical property of this coupled system changes with x.

We find the coupled system has no field-induced clustering transition if the clause density $\alpha < \alpha_d(K)$. This indicates that if we slowly increase the value of x from zero, we can reach a configuration that satisfies all the M clauses of the original system. In other words, the ran-

*Supported by the Knowledge Innovation Program of Chinese Academy of Sciences under Grant No. KJCX2-EW-J02, and the Natural National Science Foundation of China under Grant Nos. 11121403 and 11225526

dom K-SAT problem can be solved by simulated annealing on the coupling field x when $\alpha < \alpha_d(K)$. However, if $\alpha > \alpha_d(K)$ a field-induced clustering transition will occur at certain critical value of x. This indicates that when $\alpha > \alpha_d(K)$ the simulated annealing on x will have a very high probability of being trapped by one of the many ergodic domains of the coupled configuration space and fail to reach a true solution of the original formula.

We compare the temperature-induced clustering transition of the original K-SAT problem F and the coupling-induced clustering transition of the coupled system $F_1 + F_2$. We notice that the energy density at the coupling-induced clustering transition is noticeably lower than that at the temperature-induced clustering transition. This suggests that solution space coupling is an efficient approach to construct low-energy configurations for a given random K-SAT formula. If we allow the two sub-formulas F_1 and F_2 to share a subset of clauses, the simulated annealing process on x can reach configurations with even lower energy values. By properly adjusting the shared subset of clauses between sub-formulas F_1 and F_2, the solution space coupling approach might be able to solve a given random K-SAT formula even at $\alpha > \alpha_d(K)$. A stochastic search algorithm based on the solution space coupling idea was applied to the perception learning problem in an earlier paper.[18]

The paper is organized as follows. Section 2 introduces the random K-SAT problem and defines a partition function using the coupling field x as the control parameter. In Sec. 3 we study solution space coupling in the random 3-SAT and 4-SAT problems using belief-propagation iterations and simulated annealing simulations, and compare the results on single problem instances with that obtained by the replica-symmetric spin glass theory. The coupling-induced clustering phase transition is further studied in Sec. 4. We conclude our work in Sec. 5 and discuss some possible extensions. The appendices of this paper contain the analytical details of the mean-field theory.

2 The Random K-SAT Problem and Partition Functions

A random K-SAT formula F contains N variables and M clauses, with clause density $\alpha \equiv M/N$. In this paper we follow the convention in the literature and use letters $i, j, k, l, \ldots$ to denote the variables and letters $a, b, c, d, \ldots$ to denote the clauses. Each variable i has a binary spin state $\sigma_i \in \{-1, +1\}$. A collection of the spin states of all the N variables forms a configuration, denoted as $\underline{\sigma} \equiv (\sigma_1, \sigma_2, \ldots, \sigma_N)$. The total number of configurations is 2^N. Each clause a is a constraint to a subset of K randomly chosen variables from the N variables (this subset is denoted as ∂a), which disfavors a single randomly chosen spin assignment $\{-J_a^i : i \in \partial a\}$ among the 2^K possible assignments of these K variables (each $J_a^i \in \{-1, +1\}$). The energy of clause a is

$$\prod_{i \in \partial a} \frac{1 - J_a^i \sigma_i}{2}.$$

The value of this energy is zero except for the spin assignment $\{\sigma_i = -J_a^i : i \in \partial a\}$, which has unit energy. Notice that $\{J_a^i : i \in \partial a\}$ is a set of K fixed parameters specific to clause a, each J_a^i being independently setting to -1 or $+1$ with equal probability. Given a spin configuration $\underline{\sigma}$, if the energy of a clause a is zero, this clause is said to be satisfied by the configuration, otherwise clause a is said to be violated (unsatisfied) by the configuration.

Each configuration $\underline{\sigma}$ of formula F is associated with an energy $E(\underline{\sigma})$, which is the sum of the M clause energies:

$$E(\underline{\sigma}) = \sum_{a \in F} \prod_{i \in \partial a} \frac{1 - J_a^i \sigma_i}{2}. \tag{1}$$

The configuration energy $E(\underline{\sigma})$ is non-negative and integer-valued, it counts the total number of violated clauses by configuration $\underline{\sigma}$. If a configuration $\underline{\sigma}$ has zero energy, it is regarded as a solution of formula F. The solution space $\mathcal{S}$ of F is composed of all the solutions of F, namely $\mathcal{S} \equiv \{\underline{\sigma} : E(\underline{\sigma}) = 0\}$. It is convenient to represent a random K-SAT formula F by a bipartite graph with $N + M$ nodes and $K \times M$ edges.[6,19] (see Fig. 1). N of the nodes represent the variables $(i, j, k, \ldots)$ and the other M nodes represent the clauses $(a, b, c, \ldots)$. All the edges are between a variable node and a clause node: an edge (i, a) between a variable node i and a clause node a is present if (and only if) clause a involves variable i, and this edge has a coupling constant J_a^i which indicates that clause a prefers variable i to be in spin state $\sigma_i = J_a^i$.

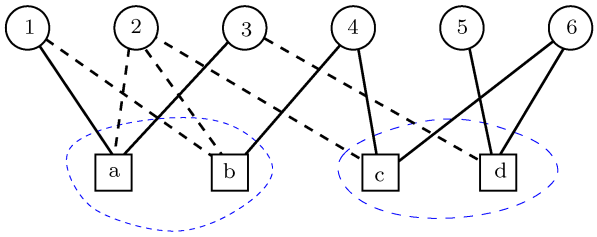

Fig. 1 The factor graph of a small 3-SAT formula with $N = 6$ variables and $M = 4$ clauses. The edge (i, a) between a variable i and a clause a is a full line if the coupling constant $J_a^i = 1$ and is a dashed line if $J_a^i = -1$. The 3-SAT formula is divided into two sub-formulas,each of them contains $M/2$ clauses.

We will refer to a random K-SAT formula F always in its bipartite graph representation. This random bipartite graph (also called a factor graph) is locally tree-like: short loops are very seldom, and typical loops have lengths at the scale of $\ln(N)$.[6,19]

Let us denote by ∂i the set of clause nodes that a variable node i is connected to. The size of this set ∂i is referred to as the degree (or connectivity) of variable i. In a random K-SAT formula with clause density α, the mean degree of a variable is $K\alpha$; when the variable number N is large enough, the probability that a randomly picked variable is connected to n clauses obeys the Poisson distribution

$$P(n) = \frac{\mathrm{e}^{-K\alpha}(K\alpha)^n}{n!}.$$

2.1 *Temperature-Related Partition Function*

A conventional partition function $\tilde{Z}(\beta)$ for studying the energy landscape of the random K-SAT problem is defined as

$$\tilde{Z}(\beta) \equiv \sum_{\underline{\sigma}} \exp[-\beta E(\underline{\sigma})]\,, \tag{2}$$

where $\beta \equiv 1/T$ is the inverse temperature (T being the temperature), and the summation is over all the 2^N possible configurations.

The statistical system (2) has been studied in many earlier papers (e.g., Refs. [9, 11, 20]). The Boltzmann factor $\mathrm{e}^{-\beta E(\underline{\sigma})}$ directly disfavors high energy configurations, and the mean energy of the system decreases with the inverse temperature β. At certain critical value $\beta = \beta_d$ an ergodicity-breaking (clustering) transition occurs in the system such that the configurations with energy density $\epsilon < \epsilon_d(K,\alpha)$ are distributed into many different configuration clusters, each of which can be regarded as a thermodynamic state of the system. The threshold energy density $\epsilon_d(K,\alpha)$ can be computed by the mean field spin glass theory.[7,21]

2.2 *Coupling-Related Partition Function*

In this work we study the energy landscape of the random K-SAT problem from another angle. Given a random K-SAT formula F, we randomly partition its clauses into two disjoint sets of equal size (M assumed to be even), see Fig. 1. Two sub-formulas F_1 and F_2 are then formed, each of which contains N variables and $(\alpha/2)N$ clauses. For any spin configuration $\underline{\sigma}$, the configuration energy of sub-formula F_1 is denoted as $E_1(\underline{\sigma})$ and that of sub-formula F_2 is denoted as $E_2(\underline{\sigma})$. Let us denote the solution space of F_1 as $\mathcal{S}_1$ and that of F_2 as $\mathcal{S}_2$, namely $\mathcal{S}_1 \equiv \{\underline{\sigma} : E_1(\underline{\sigma}) = 0\}$ and $\mathcal{S}_2 \equiv \{\underline{\sigma} : E_2(\underline{\sigma}) = 0\}$. The solution space of the whole formula F is the intersection of these two spaces, $\mathcal{S} = \mathcal{S}_1 \cap \mathcal{S}_2$.

Consider a spin configuration $\underline{\sigma}^{(1)} \in \mathcal{S}_1$ and a spin configuration $\underline{\sigma}^{(2)} \in \mathcal{S}_2$. The similarity between these two configurations is quantified by the overlap q:

$$q(\underline{\sigma}^{(1)}, \underline{\sigma}^{(2)}) = \frac{1}{N}\sum_{i=1}^{N} \sigma_i^{(1)}\sigma_i^{(2)}\,. \tag{3}$$

If the two configurations $\underline{\sigma}^{(1)}$ and $\underline{\sigma}^{(2)}$ are identical, the overlap between them achieves the maximal value 1. Let us introduce a coupling field x between the two solution spaces $\mathcal{S}_1$ and $\mathcal{S}_2$[22] and define a partition function $Z(x)$ as

$$Z(x) = \sum_{\underline{\sigma}^{(1)}\in\mathcal{S}_1} \sum_{\underline{\sigma}^{(2)}\in\mathcal{S}_2} \exp\Big(x\sum_{i=1}^{N}\sigma_i^{(1)}\sigma_i^{(2)}\Big)\,. \tag{4}$$

In the above expression, each pair of configurations $(\underline{\sigma}^{(1)}, \underline{\sigma}^{(2)})$ contributes a Boltzmann weight $\mathrm{e}^{Nxq(\underline{\sigma}^{(1)},\underline{\sigma}^{(2)})}$. Under this reweighting, the mean overlap value between a solution $\underline{\sigma}^{(1)} \in \mathcal{S}_1$ and a solution $\underline{\sigma}^{(2)} \in \mathcal{S}_2$ will be an increasing function of x. Let us denote this function as $q(x)$, it is just the first derivative of $\ln Z(x)$:

$$q(x) \equiv \frac{1}{N}\frac{\mathrm{d}}{\mathrm{d}x}\ln Z(x)\,. \tag{5}$$

If $x = 0$, the solution spaces $\mathcal{S}_1$ and $\mathcal{S}_2$ are not coupled, then $q(x = 0)$ will be the overlap value between a typical configuration of $\mathcal{S}_1$ and a typical configuration of $\mathcal{S}_2$. In the other limit of $x \to +\infty$, these two solution spaces are strongly coupled together, and the mean overlap approaches 1.

In the partition function (4), the spin configuration $\underline{\sigma}^{(1)}$ is a solution of sub-formula F_1 (namely $E_1(\underline{\sigma}^{(1)}) = 0$), but the energy $E_2(\underline{\sigma}^{(1)})$ might be positive; similarly the configuration energy $E_2(\underline{\sigma}^{(2)}) = 0$ but $E_1(\underline{\sigma}^{(2)})$ might be positive. In this paper, the energy density of the coupled system for a given pair of configurations $(\underline{\sigma}^{(1)}, \underline{\sigma}^{(2)})$ is defined as

$$\epsilon^{12}(\underline{\sigma}^{(1)}, \underline{\sigma}^{(2)}) \equiv \frac{E_2(\underline{\sigma}^{(1)}) + E_1(\underline{\sigma}^{(2)})}{2N}\,. \tag{6}$$

The statistical system (4) actually corresponds to a system of two coupled random walkers. Each random walker is restricted to moving within the solution space of one K-SAT sub-formula,[15] but they mutually affect each other due to the coupling field x. We are interested in the evolution of the statistical physics property of such a coupled system as the values of the control parameter x is changed. When the original K-SAT formula F has clause density $\alpha \approx \alpha_s(K)$, the clause density of the two sub-formulas F_1 and F_2 are still below $\alpha_d(K)$. Therefore both the solution spaces $\mathcal{S}_1$ and $\mathcal{S}_2$ are ergodic and relatively simple.[4,8,9,12,22–25]

3 Belief-Propagation and Simulated Annealing Results

We perform belief-propagation (BP) iterations on single instances of the random K-SAT problem at given values of the control parameter x for the statistical system (4). If the BP iteration process converges for a given problem instance, we compute the mean overlap value $q(x)$ and the mean energy density of the coupled system at the BP fixed point. The free energy and the entropy of the coupled system are also computed at the

BP fixed point. These BP results are compared with results obtained by simulated annealing (SA)[26−27] and the ensemble-averaged mean-field population dynamics results.

The BP iterative equations for the model (4) are listed in the appendices. The details of the SA simulation are as follows: We first construct a satisfying configuration $\underline{\sigma}^{(1)}$ for sub-formula F_1 and another satisfying configuration $\underline{\sigma}^{(2)}$ for sub-formula F_2. Then two single-spin flipping processes are simulated in the solution spaces $\mathcal{S}_1$ and $\mathcal{S}_2$, respectively.[15] These two solution space random walking processes are coupled together due to the control parameter x, which increases from $x = 0$ in steps of $\Delta x = 0.1$. The waiting time at each value of x is set to be ΔT, namely $N \times \Delta T$ flipping trials are performed for each spin-flipping process at each fixed value of x.

3.1 *The Random 3-SAT Problem*

Figure 2 collects the results obtained on the random 3-SAT problem with clause density $\alpha = 4.25$, close to the satisfiability threshold value $\alpha_s(3) = 4.267$. For the single problem instance of Fig. 2, the BP iteration is convergent when the coupling field $x < 1.92$. The results obtained by BP are in agreement with the results obtained by simulated annealing, and also in agreement with the results obtained by mean-field population dynamics. These results suggest that, when $x < 1.92$, this coupled 3-SAT system can be adequately described by the BP equations.

At $x \approx 1.92$, BP fails to converge for the single problem instance of Fig. 2. At this value of coupling constant, the mean overlap between the two solution spaces is about 0.93, that is, the configurations $\underline{\sigma}^{(1)}$ and $\underline{\sigma}^{(2)}$ only differ in about 3.5% of the vertices. The mean energy density of the two solutions is $\epsilon^{12} \approx 0.021$.

If x further increases above 1.92, although the mean overlap value and the mean energy density value as predicted by the mean-field population dynamics keep changing with x, the corresponding values as obtained by SA do not show much changing trend. This plateau behavior and the non-convergence of BP indicate a qualitative change in the statistical property of the coupled 3-SAT problem instance occurs at $x \approx 1.92$. As we will see in the next section, this qualitative change is caused by the ergodicity-breaking (clustering) transition of the coupled system. The threshold coupling field value at this phase transition (for $N \to +\infty$) is $x \approx 1.94$.

For the random 3-SAT problem at clause density $\alpha = 4.25$, the conventional partition function (2) has a temperature-induced clustering transition at the critical temperature $T_c \approx 0.23$. At this clustering transition point the energy density is $\epsilon_d(3, 4.25) \approx 0.04$, which is twice the energy density value of $\epsilon^{12} \approx 0.021$ at the coupling-induced clustering transition. This difference in the energy density levels of the temperature- and coupling field-induced ergodicity-breaking transitions suggests that, by restricting configuration $\underline{\sigma}^{(1)}$ to solution space $\mathcal{S}_1$ and $\underline{\sigma}^{(2)}$ to solution space $\mathcal{S}_2$ we can easily construct configurations for a random K-SAT formula with energy density much below $\epsilon_d(K, \alpha)$.

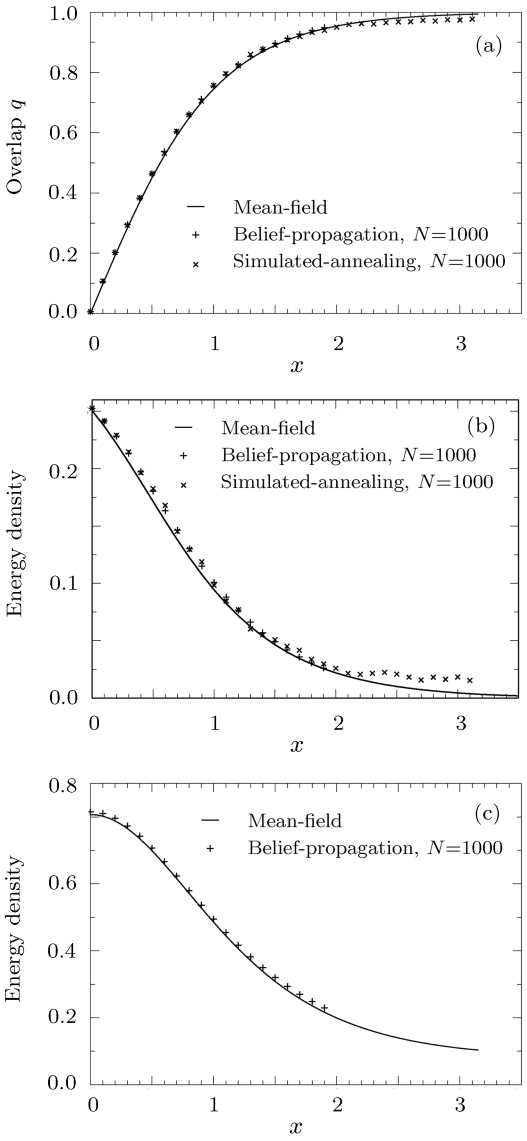

Fig. 2 The random 3-SAT problem at $\alpha = 4.25$. Mean-field population dynamics results are compared with the results obtained by BP and SA on a single small instance with $N = 10^3$ variables. (a) Mean overlap; (b) Mean energy density; (c) Entropy density. The BP iteration no longer converges at $x > 1.92$ for the single problem instance. The waiting time of SA is set to $\Delta T = 500$.

Figure 3 shows the results obtained on the random 3-SAT problem with clause density $\alpha = 3.85$, slightly below the clustering transition point $\alpha_d(3) = 3.86$. In this case, BP iteration is able to converge even at very large values of x, and the results obtained by BP are in agreement with SA results. The SA process is able to reach configurations that satisfy the whole formula F.

The results of this subsection supports the expectation

that, the coupled system has qualitative different statistical properties when the clause density α changes from $\alpha < \alpha_d(3)$ to $\alpha > \alpha_d(3)$. If $\alpha < \alpha_d(3)$, the coupled system has no clustering transition, while if $\alpha > \alpha_d(3)$ a clustering transition occurs at a finite value of x.

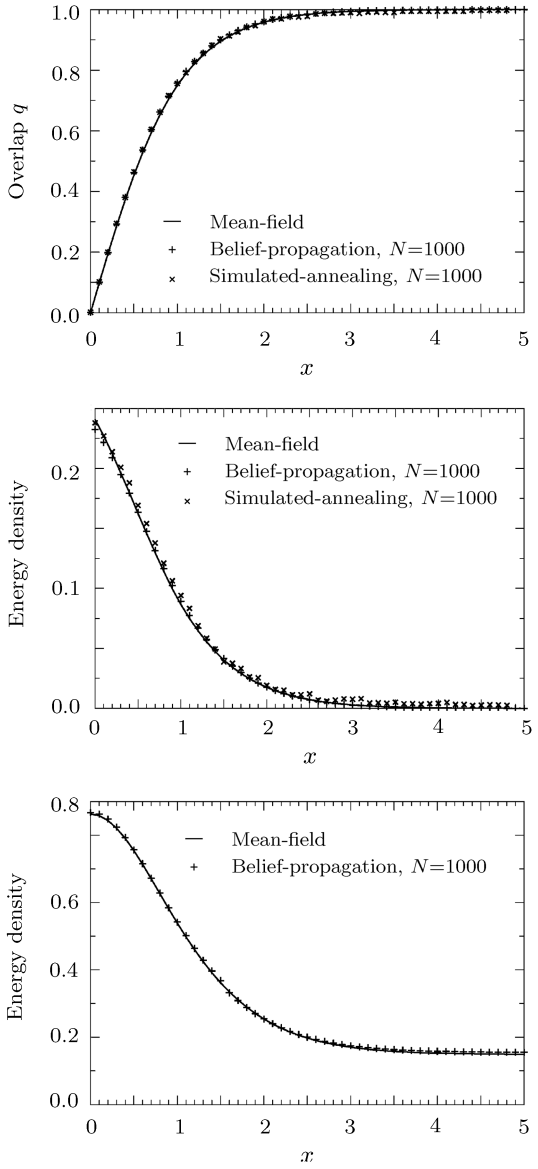

Fig. 3 Same as Fig. 2, but for the random 3-SAT problem with clause density $\alpha = 3.85$. The waiting time of SA is set to $\Delta T = 500$.

3.2 *The Random* 4*-SAT Problem*

Similar results are obtained on the random 4-SAT problem. For this problem, the value of clause density at the clustering transition is $\alpha_d(4) = 9.38$.[9,12]

The results on the coupled 4-SAT system at $\alpha = 8.5$ are shown in Fig. 4. The BP iteration is convergent, and the results obtained by BP are in agreement with the results obtained by SA and the mean-field population dynamics results. The SA process is able to reach configurations that satisfy the whole formula F.

Figure 5 shows the results obtained on the random 4-SAT problem with clause density $\alpha = 9.5$, which is larger than $\alpha_d(4)$. The BP iteration also converges on the studied single instance even for very large values of the coupling field x. However, the results obtained by BP on the mean overlap $q(x)$ are different from that obtained by SA when $x > 2.5$. As for the mean energy density, the BP predictions also deviate considerably from the results obtained by SA when $x > 2.5$. We will demonstrate in the next section that, in the thermodynamic limit $N \to \infty$, the coupled system at $\alpha = 9.5$ has a clustering transition when $x \approx 3.1$.

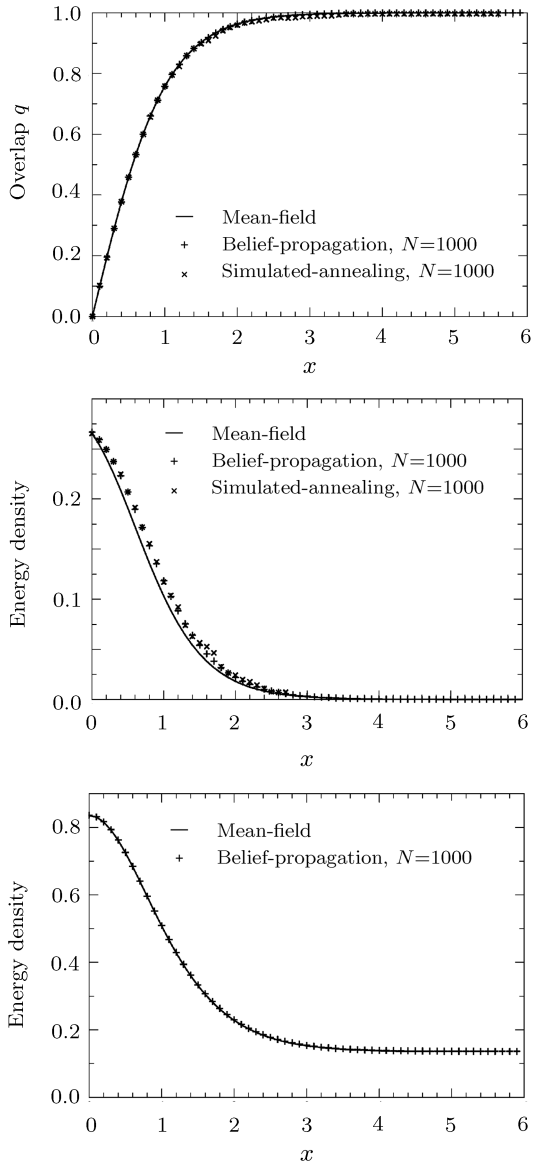

Fig. 4 Same as Fig. 2, but for the random 4-SAT problem with clause density $\alpha = 8.5$. The waiting time of SA is set to $\Delta T = 500$. The SA process reaches satisfying configuration for the whole formula at $x \approx 2.7$ and it then stops.

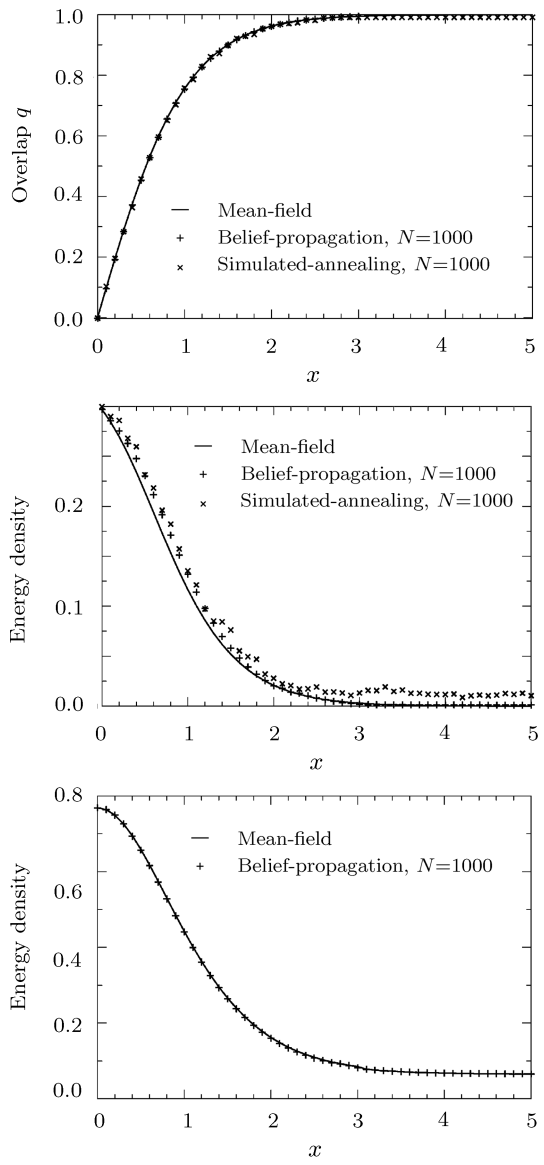

Fig. 5 Same as Fig. 2, but for the random 4-SAT problem with clause density $\alpha = 9.5$. The BP iteration is convergent but the results obtained by BP and SA do not agree with each other when $x > 2.5$. The waiting time of SA is set to $\Delta T = 1000$.

4 On the Coupling-induced Phase transition

The numerical results of the preceding section suggest that, for the random K-SAT problem with clause density $\alpha > \alpha_d(K)$, a coupling-induced phase transition will occur in the statistical model (4) at certain critical value x_d of the coupling field x. In this section, we apply the first-step replica-symmetry-breaking (1RSB) spin glass mean field theory to the partition function $Z(x)$ to determine the value of x_d. An important quantity of the 1RSB mean field theory is the complexity Σ, which is the entropy density at the level of thermodynamic states.[28] The complexity quantitatively characterizes the abundance of thermodynamic states in the system. Here we describe the main results of this theoretical calculation, while the analytical details are again deferred to the appendices. To determine the clustering transition point x_d we set the Parisi parameter of the 1RSB mean field theory to be $m = 1$.

Figure 6 shows the 1RSB results for the random 3-SAT problem with clause density $\alpha = 4.25$ (for other values of $\alpha > \alpha_d(3)$ we obtain qualitatively similar results as Fig. 6). The 1RSB theory predicts that, at the thermodynamic limit $N \to +\infty$ an ergodicity-breaking (clustering) transition occurs in the system at $x = x_d \approx 1.94$. When $x < x_d$, the complexity is $\Sigma \equiv 0$, indicating there is only one thermodynamic state (the space formed by pairs of solutions $(\underline{\sigma}^{(1)}, \underline{\sigma}^{(2)})$ is ergodic). When x increases beyond x_d, the complexity Σ becomes negative. This indicates that the system is no longer ergodic but an exponential number of thermodynamic states emerge in the configuration space. A sub-exponential number of thermodynamic states dominate the statistical property of the system at $x > x_d$. This ergodicity-breaking phase transition explains the non-convergence of BP and the plateau behavior of the SA process (the SA dynamics is no longer in equilibrium when $x > x_d$).

Figure 7 demonstrates how the critical coupling field x_d of the random 3-SAT problem changes when the clause density α increases. The value of x_d appears to diverge as $\alpha = \alpha_d(3)$. It then decreases quickly with α.

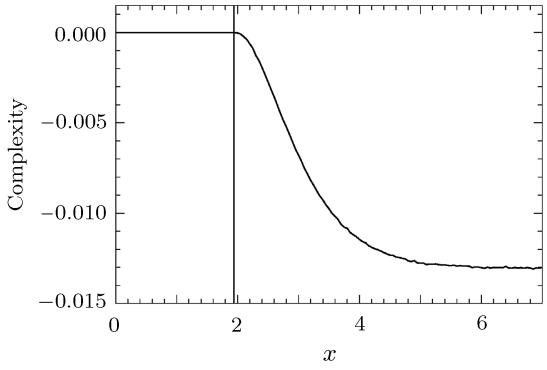

Fig. 6 Complexity Σ as a function of the coupling field x for the random 3-SAT problem with clause density $\alpha = 4.25$. The Parisi parameter is set to be $m = 1$ in the 1RSB calculations. The vertical line marks the clustering transition point of $x \approx 1.94$.

The 1RSB results for the random 4-SAT problem are shown in Fig. 8. For clause density $\alpha > \alpha_d(4)$ there is also a coupling-induced clustering transition at certain critical value x_d of the coupling field x. A qualitative difference with the coupled random 3-SAT problem is that, at $x = x_d$ the complexity Σ of the coupled random 4-SAT problem jumps from $\Sigma = 0$ to a positive value. This indicates that an exponential number of thermodynamic states are contributing to the equilibrium statistical property of the system. For the system with clause density $\alpha = 9.5$, the

clustering transition occurs at $x = x_d \approx 3.1$. The complexity value jumps to $\Sigma \approx 0.005$ at $x = x_d$; it then decreases continuously with x and reaches a limiting positive value at $x \to \infty$. At $x = x_d$ the mean energy density of the coupled system ($\alpha = 9.5$) is $\epsilon^{12} \approx 0.004$, which is about half of the energy density value $\epsilon_d(4, 9.5) \approx 0.0081$ at the temperature-induced clustering transition.

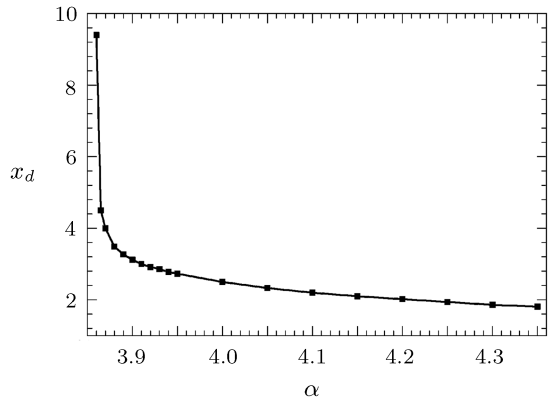

Fig. 7 Clustering transition point x_d as a function of clause density α for the random 3-SAT problem.

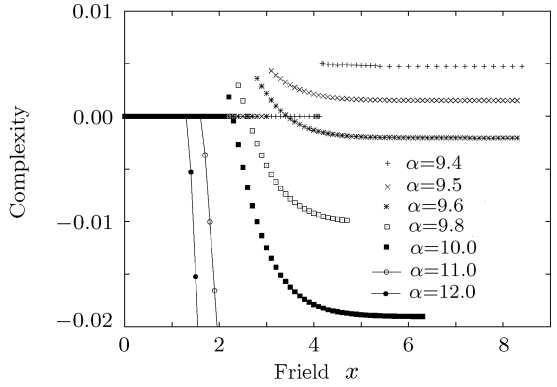

Fig. 8 The complexity for different clause density α in the coupled random 4-SAT problem. The Parisi parameter of the 1RSB mean field calculations is set to $m = 1$.

5 Conclusion and Discussion

In this paper, we studied the random K-SAT problem by dividing a K-SAT formula into two sub-formulas and applying a coupling field between the solution spaces of these two sub-formulas. We found an ergodicity-breaking (clustering) transition occurs in this coupled system at certain critical value of the coupling field x. At the coupling-induced clustering transition the energy density of the system is only about half the energy density at the temperature-induced clustering transition.

As the coupled system has an ergodicity-breaking phase transition at a finite value of x, it may not be promising to use solution space coupling as a practical algorithm for constructing a satisfying configuration for a K-SAT formula. As the value of the coupling field x slowly increases, the dynamics is likely to be trapped by a non-optimal macroscopic state, which prohibits the overlap between the two configurations from further increasing.

However, after the dynamics has been trapped by a non-optimal macroscopic state, the unsatisfied clauses by the configurations $\underline{\sigma}^{(1)}$ and $\underline{\sigma}^{(2)}$ can be identified. We can then decrease the value of x slowly and add these clauses to sub-formulas F_1 and F_2 during this process. Now sub-formulas F_1 and F_2 share some common clauses. As x further increases slowly, the dynamics for sure will not be trapped by the same non-optimal macroscopic state as before. If it is again trapped by another non-optimal macroscopic state, we can repeat the decreasing-increasing process of x to enlarge the set of shared clauses by sub-formula F_1 and F_2. This heuristic process might be able to reach a solution for the original K-SAT formula even at $\alpha > \alpha_d(K)$. It will be of interest to test this idea by extensive computer simulations.

In this work we only consider the coupling of two solution spaces. It may also be interesting to study the coupling of three or more solution spaces.

Appendix A: Belief-Propagation Equations for the Coupled random K-SATProblem

In the expression (4) for $Z(x)$, the configuration summations are restricted to the solution spaces $\mathcal{S}_1$ and $\mathcal{S}_2$, which are actually unknown to us. We now express $Z(x)$ in an alternative form which is convenient for performing a partition function expansion. Define for each variable node i a vector state $\vec{\sigma}_i \equiv (\sigma_i^{(1)}, \sigma_i^{(2)})$. The collection of the vector states of all the N variables corresponds to two spin configurations $\underline{\sigma}^{(1)}$ and $\underline{\sigma}^{(2)}$. Then, summing without any restriction over all the possible vector states of each variable node i, the partition function $Z(x)$ is expressed as

$$Z(x) = \sum_{\{\vec{\sigma}_i\}} \prod_{i=1}^{N} \psi_i(\vec{\sigma}_i) \prod_{c \in F} \psi_c(\vec{\sigma}_{\partial c}) \,. \tag{A1}$$

In the above expression, ψ_i and ψ_c are, respectively, the Boltzmann factor for variable i and clause c; $\vec{\sigma}_{\partial c}$ denotes the vector states of the variables involved in clause c, namely $\vec{\sigma}_{\partial c} \equiv \{\vec{\sigma}_i : i \in \partial c\}$. The expression for ψ_i is simply

$$\psi_i(\vec{\sigma}_i) \equiv \exp\bigl(x \sigma_i^{(1)} \sigma_i^{(2)}\bigr).$$

The Boltzmann factor for a clause, on the other hand, depends on whether the clause belongs to sub-formula F_1 or F_2: for a clause a of sub-formula F_1, its Boltzmann factor is

$$\psi_a \equiv \Bigl[1 - \prod_{j \in \partial a} \frac{1 - J_a^j \sigma_j^{(1)}}{2}\Bigr],$$

while for a clause b of sub-formula F_2, the Boltzmann factor is

$$\psi_b \equiv \Big[1 - \prod_{j\in\partial b} \frac{1 - J_b^j \sigma_j^{(2)}}{2}\Big] .$$

It is easy to check that only those configuration pairs $(\underline{\sigma}^{(1)}, \underline{\sigma}^{(2)})$ with $\underline{\sigma}^{(1)} \in \mathcal{S}_1$ and $\underline{\sigma}^{(2)} \in \mathcal{S}_2$ have non-vanishing contribution in the expression (A1).

Consider a variable node i of the random K-SAT formula F. This variable has a state $\vec{\sigma}_i$, and it is connected to a set ∂i of clauses in the K-SAT formula F, its degree being $n_i = |\partial i|$. If $n_i \geq 1$ we also introduce n_i 'image' states

$$\vec{\sigma}_{i\to c} \equiv \{\sigma_{i\to c}^{(1)}, \sigma_{i\to c}^{(2)}\}$$

for variable i, one for each clause $c \in \partial i$. All these n_i image states should all be identical to $\vec{\sigma}_i$.

Consider a clause c and its associated K variables $i \in \partial c$. Let us denote the state of such a sub-system as $\vec{\sigma}_c \equiv \{\vec{\sigma}_{i\to c} : i \in \partial c\}$, where $\vec{\sigma}_{i\to c}$ is just the image state of variable i to clause c. The total Boltzmann weight of such a sub-system is denoted as $\Psi_c(\vec{\sigma}_c)$, with

$$\Psi_c(\vec{\sigma}_c) \equiv \psi_c(\vec{\sigma}_c) \prod_{i\in\partial c} \psi_i(\vec{\sigma}_{i\to c}) . \tag{A2}$$

Regarding the n_i image states of each variable i to be independent states, the partition function expression (A1) is rewritten as

$$Z(x) = \prod_{c\in F} \Big[\sum_{\vec{\sigma}_c} \Psi_c(\vec{\sigma}_c)\Big] \prod_{i=1}^{N} \Big[\sum_{\vec{\sigma}_i} \psi_i(\vec{\sigma}_i)\Big]^{1-n_i} \times \prod_{(j,d)\in F} \Big[\delta(\vec{\sigma}_j, \vec{\sigma}_{j\to d})\Big] . \tag{A3}$$

In the above expression, (j, d) denotes an edge of the factor graph of the formula F, linking a variable node j and a clause node d; the Kronecker delta function $\delta(\vec{\sigma}_j, \vec{\sigma}_{j\to d})$ is equal to 1 if the two vector states $\vec{\sigma}_j$ and $\vec{\sigma}_{j\to d}$ are identical, otherwise its value is 0.

Let us introduce to each edge (i, c) of the factor graph of F an arbitrary probability distribution $m_{c\to i}(\vec{\sigma}_i)$, which is regarded as an estimated probability that variable i takes state $\vec{\sigma}_i$ if it is only constrained by clause c. Then it is easy to check that

$$Z(x) = \prod_{c\in F} \Big[\sum_{\vec{\sigma}_c} \Psi_c(\vec{\sigma}_c) \prod_{k\in\partial c} \prod_{a\in\partial k\backslash c} m_{a\to k}(\vec{\sigma}_{k\to c})\Big] \times \prod_{i=1}^{N} \Big[\sum_{\vec{\sigma}_i} \psi_i(\vec{\sigma}_i) \prod_{b\in\partial i} m_{b\to i}(\vec{\sigma}_i)\Big]^{1-n_i} \times \prod_{(j,d)\in F} \Big[\delta(\vec{\sigma}_j, \vec{\sigma}_{j\to d})\Big] . \tag{A4}$$

In this expression, $\partial k\backslash c$ means the set of nearest-neighboring clauses of variable node k, but with clause c being removed from this set. It is interesting to notice that the expression (A4) holds for any set of $K \times M$ arbitrary probability distributions $\{m_{c\to i}(\vec{\sigma}_i) : (i, c) \in F\}$. We can define a marginal distribution for the state $\vec{\sigma}_i$ of variable i and the state $\vec{\sigma}_c$ of clause c as

$$\omega_i(\vec{\sigma}\,) = \frac{1}{Z_i} \psi_i(\vec{\sigma}_i) \prod_{c\in\partial i} m_{c\to i}(\vec{\sigma}_i) , \tag{A5}$$

$$\omega_c(\vec{\sigma}_c) = \frac{1}{Z_c} \Psi_c(\vec{\sigma}_c) \prod_{i\in\partial c} \prod_{a\in\partial i\backslash c} m_{a\to i}(\vec{\sigma}_{i\to c}) , \tag{A6}$$

where the two normalization constants Z_i and Z_c are expressed as

$$Z_i = \sum_{\vec{\sigma}_i} \psi_i(\vec{\sigma}_i) \prod_{c\in\partial i} m_{c\to i}(\vec{\sigma}_i) , \tag{A7}$$

$$Z_c = \sum_{\vec{\sigma}_c} \Psi_c(\vec{\sigma}_c) \prod_{i\in\partial c} \prod_{a\in\partial i\backslash c} m_{a\to i}(\vec{\sigma}_{i\to c}) . \tag{A8}$$

Then Eq. (A4) is re-expressed as

$$Z(x) = Z_0 \prod_{c\in F} \Big[\sum_{\vec{\sigma}_c} \omega_c(\vec{\sigma}_c)\Big] \prod_{i=1}^{N} \Big[\sum_{\vec{\sigma}_i} \omega_i(\vec{\sigma}_i)\Big] \times \prod_{(j,d)\in F} \Big[1 + \Delta_{(j,d)}(\vec{\sigma}_j, \vec{\sigma}_{j\to d})\Big] , \tag{A9}$$

where

$$Z_0 \equiv \prod_{c\in F} Z_c \prod_{i=1}^{N} Z_i^{(1-n_i)} , \tag{A10}$$

$$\Delta_{(i,a)}(\vec{\sigma}_i, \vec{\sigma}_{i\to a}) \equiv \frac{\delta(\vec{\sigma}_i, \vec{\sigma}_{i\to a})}{\omega_i(\vec{\sigma}_i)} - 1 . \tag{A11}$$

We can expand the edge product of Eq. (A9) to obtain the following expression for $Z(x)$:

$$Z(x) = Z_0 \times \Big[1 + \sum_{f\subseteq F} L_f\Big] . \tag{A12}$$

In the above expression, f denotes a subgraph of the factor graph of formula F, which contains a set of edges (i, a) of the original factor graph and the associated variable and clause nodes; L_f is the correction contribution to the partition function by the sub-graph f, with the expression

$$L_f = \prod_{c\in f} \Big[\sum_{\vec{\sigma}_c} \omega_c(\vec{\sigma}_c)\Big] \prod_{i\in f} \Big[\sum_{\vec{\sigma}_i} \omega_i(\vec{\sigma}_i)\Big] \times \prod_{(j,d)\in f} \Delta_{(j,d)}(\vec{\sigma}_j, \vec{\sigma}_{j\to d}) . \tag{A13}$$

For a factor graph with $K \times M$ edges, the total number of non-empty subgraphs is $2^{KM} - 1$. Each of these subgraphs f contributes a term L_f to the summation of Eq. (A12). Therefore even for a moderate value of M the number of correction terms in Eq. (A12) will be exponentially large. A nice property is that a major faction of all the correction terms L_f can be made to vanish, namely $L_f = 0$.[29–31] Consider any subgraph f with a dangling edge (i, c), namely either variable node i or clause node c has no other edges connected to it within the subgraph f.

It is easy to check from Eq. (A13) that, if

$$\sum_{\vec{\sigma}_c} \omega_c(\vec{\sigma}_c)\delta(\vec{\sigma}_{i\to c},\vec{\sigma}_i) = \omega_i(\vec{\sigma}_i)\,, \tag{A14}$$

then the correction contribution of such a subgraph is $L_f = 0$. If the self-consistency condition (A14) holds on all the edges of the factor graph of formula F, then Eq. (A12) is simplified to

$$Z(x) = Z_0 \times \Big[1 + \sum_{f^{\rm loop}\subseteq F} L_{f^{\rm loop}}\Big]\,, \tag{A15}$$

where $f^{\rm loop}$ denotes a subgraph in which each node is connected by at least two edges (such a subgraph is composed purely of loops).

For a random K-SAT formula F, the typical length of a loop in its factor graph is of order $\ln N$, therefore the correction contribution $L_{f^{\rm loop}}$ of a loopy subgraph $f^{\rm loop}$ is of order $\Delta^{\ln N}$, where Δ is proportional to the mean magnitude of an edge factor $\Delta_{(i,a)}$ defined by Eq. (A11). In the case $\Delta < 1$ (which we assume), $\Delta^{\ln N} \to 0$ in the limit of $N \gg 1$. If we neglect all the loopy correction contributions of Eq. (A15), a simple approximation for the partition function is then obtained, with

$$Z(x) \approx Z_0\,. \tag{A16}$$

The self-consistent equation (A14) leads to the following belief-propagation equation for the introduced probability $m_{c\to i}(\vec{\sigma}_i)$:

$$m_{c\to i}(\vec{\sigma}_i) \propto \sum_{\{\vec{\sigma}_j : j\in\partial c\backslash i\}} \psi_c\big(\vec{\sigma}_i, \{\vec{\sigma}_j : j\in\partial c\backslash i\}\big) \times \prod_{j\in\partial c\backslash i}\Big[\psi_j(\vec{\sigma}_j)\prod_{a\in\partial j\backslash c} m_{a\to j}(\vec{\sigma}_j)\Big]\,. \tag{A17}$$

(i) ***Thermodynamic Quantities***

The set of BP equations (A17) and the partition function approximation (A16) form the replica-symmetric mean-field theory for the coupled system (4). Under this approximation, the mean overlap $q(x)$, between a solution of $\mathcal{S}_1$ and a solution of $\mathcal{S}_2$, is obtained by

$$q(x) = \frac{1}{N}\sum_{i=1}^{N}\sum_{\vec{\sigma}_i} \sigma_i^{(1)}\sigma_i^{(2)}\omega_i(\vec{\sigma}_i)\,. \tag{A18}$$

The mean energy of a configuration of $\mathcal{S}_2$ to the sub-formula F_1 is denoted as $E_1(x)$, and the mean energy of a configuration of $\mathcal{S}_1$ to the sub-formula F_2 is denoted as $E_2(x)$. The expressions for these two energies are

$$E_1(x) = \sum_{a\in F_1}\sum_{\vec{\sigma}_a}\omega_a(\vec{\sigma}_a)\prod_{i\in\partial a}\frac{1-J_a^i\sigma_i^{(2)}}{2}\,, \tag{A19}$$

$$E_2(x) = \sum_{b\in F_2}\sum_{\vec{\sigma}_b}\omega_b(\vec{\sigma}_b)\prod_{j\in\partial b}\frac{1-J_b^j\sigma_j^{(1)}}{2}\,. \tag{A20}$$

The total entropy S of the system is expressed as

$$S = \ln Z_0 - Nxq(x)\,. \tag{A21}$$

This entropy S measures the abundance of configuration pairs $(\vec{\sigma}^{(1)},\vec{\sigma}^{(2)})$ with mean overlap $q(x)$.

(ii) ***Ensemble Average by Population Dynamics***

Each clause a of the sub-formula F_1 sends out K messages $m_{a\to i}(\vec{\sigma}_i)$ to its K neighbors $i\in\partial a$. If we collect all such messages from all the $M_1 = (\alpha/2)N$ clauses of formula F_1, we obtain a large set of KM_1 messages. This set of probability distributions can be described by a probability density functional $Q_1[m(\vec{\sigma})]$, which gives the fraction of times a probability distribution $m(\vec{\sigma})$ appears in the message set. The expression for $Q_1[m(\vec{\sigma})]$ is

$$Q_1[m(\vec{\sigma})] \equiv \frac{1}{KM_1}\sum_{a\in F_1}\sum_{i\in\partial a}\delta\big(m(\vec{\sigma}) - m_{a\to i}(\vec{\sigma})\big)\,. \tag{A22}$$

The functional $Q_1[m(\vec{\sigma})]$ is normalized,

$$\int \mathcal{D}m Q_1[m(\vec{\sigma})] = 1\,,$$

where $\int\mathcal{D}$ means integration over all possible probability distributions $m(\vec{\sigma})$. A probability density functional $Q_2[m(\vec{\sigma})]$ can be constructed for the sub-formula F_2 in the same way as Eq. (A22). These two probability density functionals give a probabilistic description about the clause-to-variable messages for the random K-SAT formula F.

In the thermodynamic limit of $N\to\infty$, because of the central limit theorem, the two probability density functionals $Q_1[m(\vec{\sigma})]$ and $Q_2[m(\vec{\sigma})]$ will be independent of the structural details of the random K-SAT formula F but only depend on the clause density α and the control parameter x. Two coupled self-consistent equations for $Q_1[m(\vec{\sigma})]$ and $Q_2[m(\vec{\sigma})]$ can be easily derived after some probabilistic considerations about the local environment of a randomly chosen clause.

Let us randomly choose a clause c from sub-formula F_1, which is connected to variable i and $K-1$ other variables $j\in\partial a\backslash i$. The K edge couplings of clause c are mutually independent, each of which having equal probability to be $+1$ or -1. Each neighboring variable j of clause c might also connect to other clauses besides c. The probability $P_{nn}(k)$ that the nearest-neighbor variable j of clause c has k connections is proportional to the product of k and $P(k)$, i.e.,

$$P_{nn}(k) = \frac{kP(k)}{\sum_{k=1}^{\infty}kP(k)} = \frac{{\rm e}^{-K\alpha}(K\alpha)^{k-1}}{(k-1)!}\,,\quad k\geq 1$$

which is also a Poisson distribution but with $k\geq 1$. Each of the $k-1$ other connected clauses of the variable j has equal probability to belong to sub-formula F_1 and to sub-formula F_2. Therefore, the probability that message from clause c to variable i being equal to $m(\vec{\sigma}_i)$ is calculated to be

$$Q_1[m(\vec{\sigma}_i)] = \frac{1}{2^K}\sum_{J_c^i=\pm1}\prod_{j=1}^{K-1}\Big[\sum_{J_c^j=\pm1}\prod_{k_j=1}^{+\infty}P_{nn}(k_j)$$

$$\times \prod_{b=1}^{k_j-1} \int \mathcal{D}m_{b\to j}\Big(\frac{Q_1[m_{b\to j}]}{2}+\frac{Q_2[m_{b\to j}]}{2}\Big)\Big] \times \delta\Big(m(\vec{\sigma}_i)-m_{c\to i}(\vec{\sigma}_i)\Big)\,, \tag{A23}$$

where the expression for the probability distribution $m_{c\to i}(\vec{\sigma}_i)$ is given by Eq. (A17) with clause c belonging to sub-formula F_1. A similar self-consistent equation can be written down for $Q_2[m(\vec{\sigma}_i]$ but with clause c being chosen from sub-formula F_2.

The self-consistent equation (A23) can be solved by population dynamics simulations[6−7,32] as commonly used in the literature. Based on the two probability density functionals $Q_1[m(\vec{\sigma}\,)]$ and $Q_2[m(\vec{\sigma}\,)]$, the mean overlap value and the densities of the other thermodynamic quantities mentioned in Appendix A1 can all be calculated. These ensemble-averaged results can be compared with the results obtained on a single problem instance by the BP iteration process.

Appendix B: Details of the 1-RSB Calculation at Parisi Parameter $m = 1$

First, standard belief propagation method is applied and the messages are defined similarly. $p_{i\to c}(\sigma_i^{(1)},\sigma_i^{(2)})$ is the cavity probability that vertex i is in the state $(\sigma_i^{(1)},\sigma_i^{(2)})$ in the absence of c, one of its neighboring constraints (we use the index c to represent any clause belonging to F_1 or F_2):

$$p_{i\to c}(\sigma_i^{(1)},\sigma_i^{(2)}) = \frac{1}{Z_{i\to c}}\exp(x\sigma_i^{(1)}\sigma_i^{(2)}) \prod_{a\in\partial i\backslash c}\Big(1-\delta^{-J_a^i}_{\sigma_i^{(1)}}\prod_{j\in\partial a\backslash i}\sum_{\sigma} p_{j\to a}(-J_a^j,\sigma)\Big) \times \prod_{b\in\partial i\backslash c}\Big(1-\delta^{-J_b^i}_{\sigma_i^{(2)}}\prod_{j\in\partial b\backslash i}\sum_{\sigma} p_{j\to b}(\sigma,-J_b^j)\Big) \equiv \mathcal{F}_{RS}\,. \tag{A24}$$

where δ_m^n is the Kronecker symbol ($\delta_m^n = 1$ if $m = n$ and $\delta_m^n = 0$ if $m \neq n$), and a denotes a clause belonging to F_1 and b denotes a clause belonging to F_2. Once reaching the fixed point, the mean overlap $\bar{q}(x)$ and the entropy density $s(q)$ both can be calculated.

Then, the 1RSB description is like this:

$$\psi_{i\to c}(p_{i\to c}) = \frac{1}{\mathcal{Z}_{i\to c}}\int \prod_{a\in\partial i\backslash c}\prod_{j\in\partial a\backslash i}\mathrm{d}\psi_{j\to a}(p_{j\to a}) \prod_{b\in\partial i\backslash c}\prod_{j\in\partial b\backslash i}\mathrm{d}\psi_{j\to b}(p_{j\to b})\delta(p_{i\to c}-\mathcal{F}_{RS})\,\mathrm{e}^{-y\Delta F_{i\to c}}\,. \tag{A25}$$

We denote the distribution of $p_{i\to c}$ among all the Gibbs stats by $\psi_{i\to c}(p_{i\to c})$ and define $\bar{p}_{i\to c}(\sigma_i^{(1)},\sigma_i^{(2)})$ as the average probability,

$$\bar{p}_{i\to c}(\sigma_i^{(1)},\sigma_i^{(2)}) = \int \mathrm{d}\psi_{i\to c}(p_{i\to c})p_{i\to c}(\sigma_i^{(1)},\sigma_i^{(2)})\,. \tag{A26}$$

It is easy to see that this average probability obeys the same iterative equations as $p_{i\to c}$ (Eq. (A24)). To get rid of the reweighting factor in the self-consistence equation Eq. (A25), we define a conditional probability when the value of the spin pair is $(\sigma_i^{(1)},\sigma_i^{(2)})$ and the mean probability $\bar{p}_{i\to c}$ is given.

$$\psi_{i\to c}^{(\sigma_i^{(1)},\sigma_i^{(2)})}(p_{i\to c}|\bar{p}_{i\to c}) \equiv \frac{\psi_{i\to c}(p_{i\to c})p_{i\to c}(\sigma_i^{(1)},\sigma_i^{(2)})}{\bar{p}_{i\to c}(\sigma_i^{(1)},\sigma_i^{(2)})} = \int \prod_{a\in\partial i\backslash c}\sum_{\{\sigma_j^{(1)},\sigma_j^{(2)}\}}\mu_a^{(\sigma_i^{(1)},\sigma_i^{(2)})}\prod_{j\in\partial a\backslash i}\mathrm{d}\psi_{j\to a}^{(\sigma_j^{(1)},\sigma_j^{(2)})} \times \prod_{b\in\partial i\backslash c}\sum_{\{\sigma_j^{(1)},\sigma_j^{(2)}\}}\nu_b^{(\sigma_i^{(1)},\sigma_i^{(2)})}\prod_{j\in\partial b\backslash i}\mathrm{d}\psi_{j\to b}^{(\sigma_j^{(1)},\sigma_j^{(2)})}\delta(p_{i\to c}-\mathcal{F}_{RS})\,, \tag{A27}$$

where the summation runs over all the configuration of $(\sigma_j^{(1)},\sigma_j^{(2)})$. $\mu_a^{(\sigma_i^{(1)},\sigma_i^{(2)})}(\underline{\sigma}_{\partial a\backslash i})$ (resp. $\nu_b^{(\sigma_i^{(1)},\sigma_i^{(2)})}(\underline{\sigma}_{\partial b\backslash i})$) is the probability of a satisfying spin assignment $\underline{\sigma}_{\partial a\backslash i}$ (resp. $\underline{\sigma}_{\partial b\backslash i}$) for constraint a (resp. b) given the spin pair value $(\sigma_i^{(1)},\sigma_i^{(2)})$ of the vertex i.

The grand free energy density g of this system can be represented by the grand free energy increase caused by vertex i, constraint a and b. It has the following expression at $m = 1$:

$$g = \frac{1}{N}\sum_{i=1}^{N}\Delta G_i - \frac{1}{N}\sum_{a=1}^{\alpha_1 N}(K-1)\Delta G_a - \frac{1}{N}\sum_{b=1}^{\alpha_2 N}(K-1)\Delta G_b\,,$$

$$\mathrm{e}^{-y\Delta G_i} = \prod_{a\in\partial i}\prod_{j\in\partial a\backslash i}\int \mathrm{d}p_{j\to a}\psi_{j\to a}(p_{j\to a}) \prod_{b\in\partial i}\prod_{j\in\partial b\backslash i}\int \mathrm{d}p_{j\to b}\psi_{j\to b}(p_{j\to b})\,\mathrm{e}^{-y\Delta F_i}$$

$$= \sum_{\sigma_i^{(1)}} \sum_{\sigma_i^{(2)}} \exp(x\sigma_i^{(1)}\sigma_i^{(2)}) \prod_{a\in\partial i} \left[1 - \delta_{\sigma_i^{(1)}}^{-J_a^i} \prod_{j\in\partial a\backslash i} \sum_{\sigma} \bar{p}_{j\to a}(-J_a^j, \sigma)\right] \prod_{b\in\partial i} \left[1 - \delta_{\sigma_i^{(2)}}^{-J_b^i} \prod_{j\in\partial b\backslash i} \sum_{\sigma} \bar{p}_{j\to b}(\sigma, -J_b^j)\right],$$

$$\mathrm{e}^{-y\Delta G_a} = \int \mathrm{d}p_{j\to a}\psi_{j\to a}(p_{j\to a})\,\mathrm{e}^{-y\Delta F_a} = 1 - \prod_{j\in\partial a} \sum_{\sigma} \bar{p}_{j\to a}(-J_a^j, \sigma),$$

$$\mathrm{e}^{-y\Delta G_b} = \int \mathrm{d}p_{j\to b}\psi_{j\to b}(p_{j\to b})\,\mathrm{e}^{-y\Delta F_b} = 1 - \prod_{j\in\partial b} \sum_{\sigma} \bar{p}_{j\to b}(\sigma, -J_b^j). \tag{A28}$$

The mean free energy density $\bar{f}$ is expressed as

$$\bar{f} = \frac{1}{N}\sum_{i=1}^{N} \overline{\Delta F}_i - \frac{1}{N}\sum_{a=1}^{\alpha_A N} (K-1)\overline{\Delta F_a} - \frac{1}{N}\sum_{b=1}^{\alpha_B N} (K-1)\overline{\Delta F_b}, \tag{A29}$$

where $\overline{\Delta F}_i$, $\overline{\Delta F_a}$ and $\overline{\Delta F_b}$ are respectively the mean free energy increase caused by vertex i, constraint a and b. $\overline{\Delta F}_i$ has the following expression at $m = 1$:

$$\overline{\beta\Delta F_i} = -\frac{\int \prod_{a\in\partial i}\prod_{j\in\partial a\backslash i} \mathrm{d}\psi_{j\to a} \prod_{b\in\partial i}\prod_{j\in\partial b\backslash i} \mathrm{d}\psi_{j\to b} Z_i \log Z_i}{\int \prod_{a\in\partial i}\prod_{j\in\partial a\backslash i} \mathrm{d}\psi_{j\to a} \prod_{b\in\partial i}\prod_{j\in\partial b\backslash i} \mathrm{d}\psi_{j\to b} Z_i},$$

$$Z_i = \sum_{\sigma_i^{(1)}} \sum_{\sigma_i^{(2)}} \mathrm{e}^{x\sigma_i^{(1)}\sigma_i^{(2)}} \prod_{a\in\partial i} \sum_{\{\sigma_j^{(1)},\sigma_j^{(2)}\}} w_a \prod_{j\in\partial a\backslash i} p_{j\to a} \prod_{b\in\partial i} \sum_{\{\sigma_j^{(1)},\sigma_j^{(2)}\}} w_b \prod_{j\in\partial b\backslash i} p_{j\to b},$$

where w_a (resp. w_b) takes the value 1 if a (resp. b) is satisfied otherwise equals 0. By inserting the conditional probability Eq. (A27), it can be expressed as following:

$$\overline{\beta\Delta F_i} = -\sum_{\sigma_i^{(1)}} \sum_{\sigma_i^{(2)}} \bar{p}_i(\sigma_i^{(1)}, \sigma_i^{(2)}) \int \prod_{a\in\partial i} \sum_{\{\sigma_j^{(1)},\sigma_j^{(2)}\}} \mu_a^{(\sigma_i^{(1)},\sigma_i^{(2)})} \mathrm{d}\psi_{j\to a}^{(\sigma_j^{(1)},\sigma_j^{(2)})} \prod_{b\in\partial i} \sum_{\{\sigma_j^{(1)},\sigma_j^{(2)}\}} \nu_b^{(\sigma_i^{(1)},\sigma_i^{(2)})} \mathrm{d}\psi_{j\to b}^{(\sigma_j^{(1)},\sigma_j^{(2)})} \log Z_i.$$

Similarly,

$$\overline{\beta\Delta F_a} = \sum_{\underline{\sigma}_{\partial a}^{(1)}} \sum_{\underline{\sigma}_{\partial a}^{(2)}} \mu_a(\underline{\sigma}_{\partial a}) \int \prod_{j\in\partial a} \mathrm{d}\psi_{j\to a}^{(\sigma_j^{(1)},\sigma_j^{(2)})} \log Z_a, \quad \overline{\beta\Delta F_b} = \sum_{\underline{\sigma}_{\partial b}^{(1)}} \sum_{\underline{\sigma}_{\partial b}^{(2)}} \nu_b(\underline{\sigma}_{\partial b}) \int \prod_{j\in\partial a} \mathrm{d}\psi_{j\to b}^{(\sigma_j^{(1)},\sigma_j^{(2)})} \log Z_b,$$

where μ_a (resp. ν_b) is the probability of a satisfying spin assignment $\underline{\sigma}_{\partial a}$ (resp. $\underline{\sigma}_{\partial b}$) for constraint a (resp. b) given the spin pair value $(\sigma_i^{(1)}, \sigma_i^{(2)})$ of the vertex i. The complexity $\Sigma(m = 1)$ is related to g and $\bar{f}$, $\Sigma(m = 1) = -yg + y\bar{f}$. Now all these quantities can be calculate by the distribution of $\bar{p}_{i\to c}$ and $\psi_{i\to c}^{(\sigma_i^{(1)},\sigma_i^{(2)})}(p_{i\to c}|\bar{p}_{i\to c})$ which can be regarded as a just one-dimensional population.

Acknowledgments

Y. Zeng thanks Chuang Wang for helpful discussions.

References

[1] S.A. Cook, in *Proceedings of the Third Annual ACM Symposium on Theory of Computing*, ACM, New York (1971) pp. 151-58.

[2] P. Cheeseman, B. Kanefsky, and W. Taylor, in *Proceedings 12th Int. Joint Conf. on Artificial Intelligence*, Morgan Kaufmann Publishers Inc., San Francisco, CA, USA **1** (1991) pp. 163-69.

[3] S. Kirkpatrick and B. Selman, Science **264** (1994) 1297.

[4] R. Monasson and R. Zecchina, Phys. Rev. Lett. **76** (1996) 3881.

[5] M. Mézard, G. Parisi, and R. Zecchina, Science **297** (2002) 812.

[6] M. Mézard and A. Montanari, *Information, Physics, and Computation*, Oxford Universty Press, New York (2009).

[7] M. Mézard and G. Parisi, Eur. Phys. J. B **20** (2001) 217.

[8] M. Mézard and R. Zecchina, Phys. Rev. E **66** (2002) 056126.

[9] F. Krzaka la, A. Montanari, F. Ricci-Tersenghi, G. Semerjian, and L. Zdeborová, Proc. Natl. Acad. Sci. **104** (2007) 10318.

[10] S. Mertens, M. Mézard, and R. Zecchina, Rand. Struct. Algorithms **28** (2006) 340.

[11] H.J. Zhou, Phys. Rev. E **77** (2008) 066102.

[12] A. Montanari, F. Ricci-Tersenghi, and G. Semerjian, Journal of Statistical Mechanics: Theory and Experiment **2008** (2008) P04004.

[13] F. Krzakala and J. Kurchan, Phys. Rev. E **76** (2007) 021122.

[14] M. Alava, J. Ardelius, E. Aurell, P. Kaski, S. Krishnamurthy, P. Orponen, and S. Seitz, Proc. Natl. Acad. Sci. USA **105** (2008) 15253.

[15] H. Zhou, Eur. Phys. J. B **73** (2010) 617.

[16] J. Ardelius and L. Zdeborova, Phys. Rev. E **78** (2008) 040101(R).
[17] G. Semerjian, J. Stat. Phys. **130** (2008) 251.
[18] H.P. Huang and H.J. Zhou, Europhys. Lett. **96** (2011) 58003.
[19] A.K. Hartmann and W. Weigt, *Phase Transitions in Combinatorial Optimization Problems*, Wiley-VCH, Weinheim, Germany (2005).
[20] A. Montanari, G. Parisi, and F. Ricci-Tersenghi, J. Phys. A: Math. Gen. **37** (2004) 2073.
[21] M. Mézard and A. Montanari, J. Stat. Phys. **124** (2006) 1317.
[22] H. Zhou and C. Wang, J. Stat. Mech.: Theory and Exp. **2010** (2010) P10010.
[23] K. Li, H. Ma, and H. Zhou, Phys. Rev. E **79** (2009) 031102.
[24] H. Zhou and H. Ma, Phys. Rev. E **80** (2009) 066108.
[25] H. Zhou, J. Phys.: Conf. Series **233** (2010) 012011.
[26] S. Kirkpatrick, C.D. Gelatt, and M.P. Vecchi, Science **220** (1983) 671.
[27] V. Černý, J. Optimiz. Theor. Appl. **45** (1985) 41.
[28] R. Monasson, Phys. Rev. Lett. **75** (1995) 2847.
[29] J.Q. Xiao and H. Zhou, J. Phys. A: Math. Theor. **44** (2011) 425001.
[30] H. Zhou, C. Wang, J.Q. Xiao, and Z. Bi, J. Stat. Mech.: Theor. Exp. (2011) L12001.
[31] H. Zhou and C. Wang, J. Stat. Phys. **148** (2012) 513.
[32] R. Abou-Chacra, P.W. Anderson, and D.J. Thouless, J. Phys. C: Solid Stat Phys. **6** (1973) 1734.